NASA/TM-20220017773

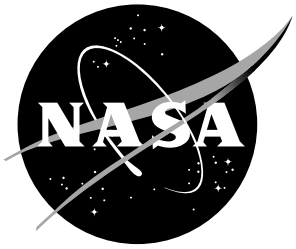

Implementation of the NASA High Intensity Modal Impedance Tube

Michael G. Jones, Alexander N. Carr, Douglas M. Nark
Langley Research Center, Hampton, Virginia

Lawrence E. Becker
Analytical Services & Materials, Hampton, Virginia

December 2022

NASA STI Program. . . in Profile

Since its founding, NASA has been dedicated to the advancement of aeronautics and space science. The NASA scientific and technical information (STI) program plays a key part in helping NASA maintain this important role.

The NASA STI Program operates under the auspices of the Agency Chief Information Officer. It collects, organizes, provides for archiving, and disseminates NASA's STI. The NASA STI Program provides access to the NASA Aeronautics and Space Database and its public interface, the NASA Technical Report Server, thus providing one of the largest collection of aeronautical and space science STI in the world. Results are published in both non-NASA channels and by NASA in the NASA STI Report Series, which includes the following report types:

- TECHNICAL PUBLICATION. Reports of completed research or a major significant phase of research that present the results of NASA programs and include extensive data or theoretical analysis. Includes compilations of significant scientific and technical data and information deemed to be of continuing reference value. NASA counterpart of peer-reviewed formal professional papers, but having less stringent limitations on manuscript length and extent of graphic presentations.
- TECHNICAL MEMORANDUM. Scientific and technical findings that are preliminary or of specialized interest, e.g., quick release reports, working papers, and bibliographies that contain minimal annotation. Does not contain extensive analysis.
- CONTRACTOR REPORT. Scientific and technical findings by NASA-sponsored contractors and grantees.
- CONFERENCE PUBLICATION. Collected papers from scientific and technical conferences, symposia, seminars, or other meetings sponsored or co-sponsored by NASA.
- SPECIAL PUBLICATION. Scientific, technical, or historical information from NASA programs, projects, and missions, often concerned with subjects having substantial public interest.
- TECHNICAL TRANSLATION. English-language translations of foreign scientific and technical material pertinent to NASA's mission.

Specialized services also include organizing and publishing research results, distributing specialized research announcements and feeds, providing information desk and personal search support, and enabling data exchange services.

For more information about the NASA STI Program, see the following:

- Access the NASA STI program home page at `http://www.sti.nasa.gov`
- E-mail your question to `help@sti.nasa.gov`
- Phone the NASA STI Information Desk at 757-864-9658
- Write to:
  NASA STI Information Desk
  Mail Stop 148
  NASA Langley Research Center
  Hampton, VA 23681-2199

NASA/TM-20220017773

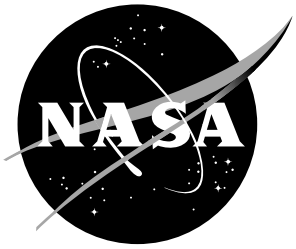

Implementation of the NASA High Intensity Modal Impedance Tube

Michael G. Jones, Alexander N. Carr, Douglas M. Nark
Langley Research Center, Hampton, Virginia

Lawrence E. Becker
Analytical Services & Materials, Hampton, Virginia

National Aeronautics and
Space Administration

Langley Research Center
Hampton, Virginia 23681-2199

December 2022

Acknowledgments

This work was funded by the Advanced Air Transport Technology Project of the NASA Advanced Air Vehicles Program. The authors wish to express their appreciation to Brian Howerton and Chelsea Solano of the Structural Acoustics Branch, Alonzo (Max) Reid and Martha Brown of the Aeroacoustics Branch, and Ayman Abdelraham of Analytical Services & Materials for their support in bringing this new test capability online.

Available from:

NASA STI Program / Mail Stop 148
NASA Langley Research Center
Hampton, VA 23681-2199
Fax: 757-864-6500

Abstract

This paper provides a description of the High Intensity Modal Impedance Tube (HIMIT) and its use for the evaluation of acoustic liners. Tests conducted with two liners, one linear and one nonlinear, are used to evaluate the suitability of the HIMIT for evaluation at frequencies up to 6 kHz and sound pressure levels up to 155 dB. Two impedance eduction methods are used, one suitable for plane wave frequencies and the other applicable over the full frequency range. These educed impedances are compared against those computed with an impedance prediction method and against those educed with another zero-flow test rig. These results confirm that the HIMIT can be used with confidence for the evaluation of acoustic liners over these frequency and sound pressure level ranges.

1 Introduction

Acoustic liners are typically mounted in the walls of the inlet and aft bypass duct of aircraft engine nacelles to reduce the amount of fan noise that is radiated to surrounding communities. The aeroacoustic environment in these engines can be quite harsh. Near the fan face, this envinronment includes mean flow up to transonic speeds, sound pressure levels (SPL) approaching 170 dB, and frequency content up to 10 kHz.

The NASA Langley Liner Physics Team has implemented multiple test rigs in the Liner Technology Facility to evaluate acoustic liners. The Normal Incidence Tube (NIT) is used to evaluate acoustic liners at SPLs up to about 150 dB and frequencies up to 3 kHz, while the Grazing Flow Impedance Tube includes the effects of mean flow up to Mach 0.6. A larger flow duct, the Curved Duct Test Rig, allows evaluation of the effects of higher-order modes on the sound absorption properties of acoustic liners. While these measurement capabilities are extensive, there is a need to extend them further.

This report documents the implementation of a new test rig, labeled the High Intensity Modal Impedance Tube (HIMIT), that was recently brought online in the Liner Technology Facility. The HIMIT is designed to evaluate acoustic liners at SPLs up to 170 dB and frequencies up to 6 kHz, albeit in a zero-flow environment. Data acquired with two carefully selected acoustic liners is used to demonstrate the ability of the HIMIT to achieve these goals, and also to demonstrate the efficacy of the methods used to evaluate these liners.

There are a few test rigs with a subset of these capabilities but, to the authors' knowledge, the HIMIT provides a unique capability for testing in this aeroacoustic environment. Lympany et al. [1] describes a transmission loss waveguide designed to achieve 150 dB at frequencies up to 4.5 kHz and for temperatures up to 260° C. They employed a modal decomposition approach to measure acoustic performance. Khodashenas et al. [2] presents results acquired in a normal incidence tube with SPLs up to 150 dB at frequencies up to 1.7 kHz. Their duct diameter was sufficiently small such that only plane waves were present. Similarly, Palani et al. [3] present results from a duct with even smaller diameter such that they are able to test up to 5.5 kHz with only plane waves.

The remainder of the paper is organized as follows. Section 2 provides descriptions of the HIMIT and test liners. Section 3 presents the analysis tools used to validate the HIMIT operation. Initial results are provided in Section 4, followed by some concluding remarks in Section 5.

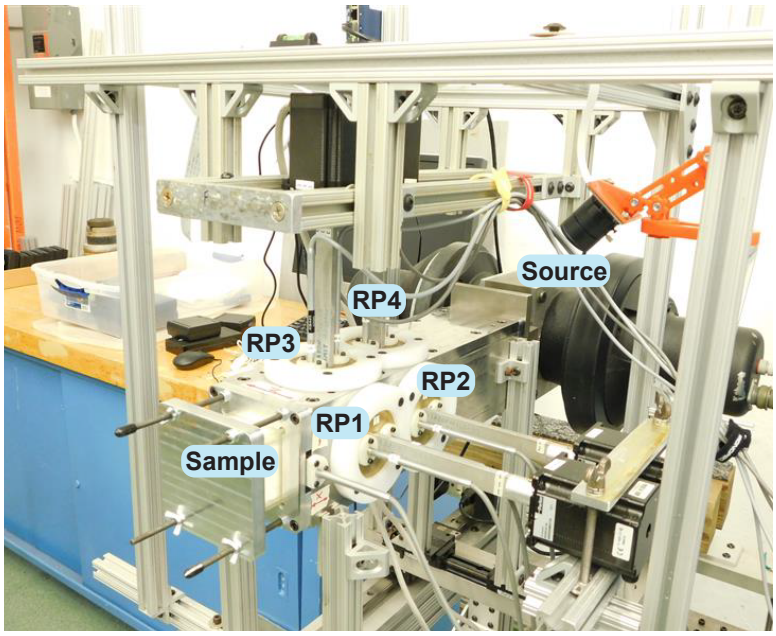

Figure 1: NASA Langley High Intensity Modal Impedance Tube.

2 Experimental Method

This section contains a description of the HIMIT and the two acoustic liners used to evaluate the capabilities of this test rig.

2.1 High Intensity Modal Impedance Tube (HIMIT)

The NASA Langley High Intensity Modal Impedance Tube (HIMIT, Fig. 1) is a zero-flow, $2.0'' \times 2.0''$ waveguide designed to measure the acoustic impedance of aircraft liner samples. Sound can be injected into the HIMIT using one of two options: (1) two compression drivers (as shown in the photograph) or (2) a Hartmann generator. The current report will be confined to the operation of the HIMIT using the two compression drivers.

The injected sound propagates down the $14''$-long waveguide to the surface of the acoustic liner, where it is reflected to set up an acoustic pressure standing wave. A $0.25''$-diameter reference microphone mounted $0.25''$ from the liner surface is used to determine the total SPL at the surface of the acoustic liner. The excitation voltage fed to the acoustic drivers is adjusted on a per frequency basis to ensure that the acoustic liner is evaluated at the same SPL for each test frequency.

Eight $0.125''$-diameter measurement microphones are mounted in four rotating plugs (labeled as RP1 — RP4), two on the upper wall and two on the right wall (looking from left to right in Fig. 1). Each of these microphones has a frequency-independent response over a frequency range extending well beyond that used in this study. These measurement microphones are used to measure the acoustic pressures at prescribed distances from the liner surface. When the test frequency is sufficiently low that no higher-order modes are cut on (i.e., up to approximately 3.4 kHz), the

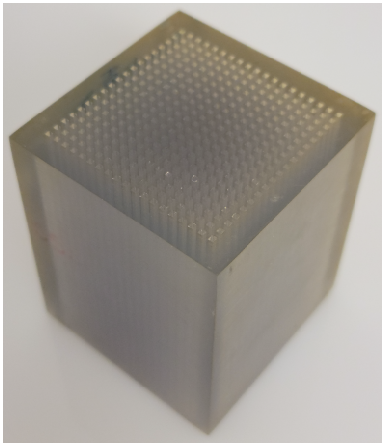

(a) Photograph of CSQ3 calibration liner.

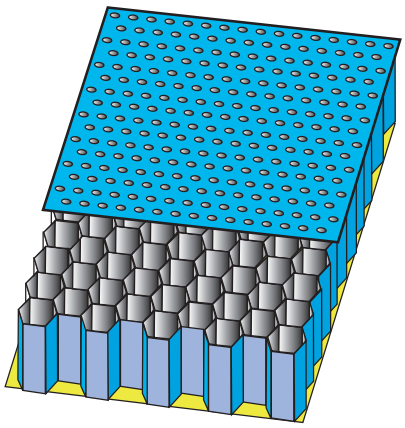

(b) Sketch of GE01 conventional liner.

Figure 2: Depictions of test liners.

data can be processed using the Two-Microphone Method (TMM) [4] to determine the frequency dependence of the acoustic impedance of the liner. Further, this process can be achieved with a single microphone if that microphone is sequentially positioned to two properly chosen locations [5].

For frequencies where higher-order modes are present, data acquired with each of the eight measurement microphones are used with a modal decomposition analysis to determine the distribution of power between the modes and the propagation constant for each of these modes. At the highest frequency considered in the current study, the [0,0], [1,0], [0,1], and [1,1] modes are cut on.[1] This information is used to compute an impedance for each mode.

2.2 Test Liners

Two acoustic liners are used in this initial evaluation of the HIMIT capabilities. The first, labeled CSQ3 (Fig. 2a), is an additively manufactured sample that consists of a 19×19 array of $0.05'' \times 0.05''$ chambers, where each chamber has a total length of $3''$. Because of the large length to diameter ratio of these chambers, this sample is very linear (insensitive to changes in acoustic particle velocity) and is thus ideal as a calibration liner.

The second, labeled GE01 (Fig. 2b), is a conventional perforate-over-honeycomb liner that has been previously evaluated on numerous occasions [6, 7]. As is common for this type of liner, the GE01 liner is considered to be weakly nonlinear, and therefore, is much more dependent on the acoustic particle velocity (and hence, the SPL) of the sound field at the liner surface. The GE01 liner facesheet is $0.025''$ thick with $0.039''$-diameter holes and an open area ratio of 0.087. This facesheet is mounted over a $1.5''$-deep phenolic core consisting of $0.75''$-wide hexagonal chambers.

[1] Modes are presented in $[n, m]$ format, where n and m are the horizontal and vertical mode orders, respectively.

3 Analysis

This section presents a brief description of the ZKTL impedance prediction model, a transmission line model based on the derivation for sound propagation in narrow chambers presented by Zwikker and Kosten [8]. It also presents brief descriptions of the methods used to process HIMIT data.

3.1 Impedance prediction model

A simplified version of the NASA Zwikker and Kosten Transmission Line (ZKTL) impedance prediction code [9,10] is used to predict the surface impedance for the CSQ3 calibration liner. This liner consists of identical chambers that are replicated to form the entire liner. Each of these chambers consists of a single air gap that is assumed to be terminated with a rigid backplate. Given the small cross-sectional dimensions of these chambers, no facesheet is needed.

The analysis is initiated by assuming the backplate to be rigid and impervious to sound, with acoustic pressure and particle velocity given by

$$\begin{pmatrix} p_0 \\ u_0 \end{pmatrix} = \begin{pmatrix} 1 \\ 0 \end{pmatrix}. \tag{1}$$

Changes in normalized acoustic pressure, p, and particle velocity, u, across the air gap are given by

$$\begin{pmatrix} p_1 \\ u_1 \end{pmatrix} = \begin{pmatrix} B_{11} & B_{12} \\ B_{21} & B_{22} \end{pmatrix} \begin{pmatrix} p_0 \\ u_0 \end{pmatrix}. \tag{2}$$

The transmission coefficients are

$$B_{11} = B_{22} = \cosh(k\Gamma H);\ B_{12} = \zeta_c \sinh(k\Gamma H);\ B_{21} = \zeta_c^{-1} \sinh(k\Gamma H), \tag{3}$$

and the acoustic pressure and particle velocity are normalized by the quantities ρc^2 and c, respectively. Here, ρ is the density, c is the sound speed, k is the freespace wavenumber, Γ is the propagation constant, ζ_c is the characteristic impedance, and H is the height of the air gap. The impedance ζ_1 at the top of the first chamber is given by $\zeta_1 = p_1/u_1$. This process is conducted for each chamber of the full liner. The surface impedance spectra ζ_n of the individual chambers are then combined to compute the effective impedance ζ_s across the liner surface using

$$\zeta_s = \theta + i\,\chi = \left[\Omega \sum_{i=1}^{N_{ch}} (\zeta_n)^{-1} \right]^{-1}, \tag{4}$$

where Ω is the open area ratio and N_{ch} is the number of chambers (361 for the CSQ3 sample).

3.2 Modal Analysis and Impedance Computation

As shown in Figure 3, the HIMIT is a waveguide with an acoustic source at one end, rigid side walls, and a finite impedance boundary condition at the other end. The width and height of the duct are W and H, respectively. The incident wave travels in the $-x$ direction until it reaches the sample and is reflected in the x direction.

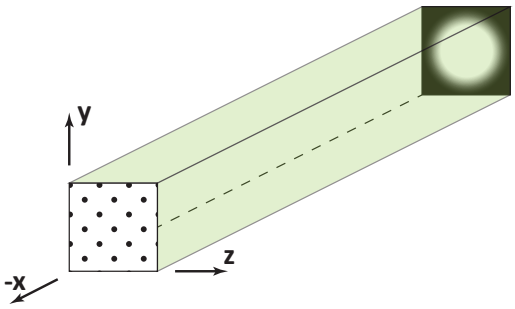

Figure 3: Coordinate system for mode decomposition.

The governing equation of the acoustic pressure, p, in a duct with no flow is

$$\frac{1}{c^2}\frac{\partial^2 p}{\partial t^2} - \nabla^2 p = 0. \tag{5}$$

If we assume $p(x,y,z,t) = \mathcal{R}\left[A(k_x,k_y,k_z,\omega)\exp(i\mathbf{k}\cdot\mathbf{r})\exp(i\omega t)\right]$, we obtain the dispersion relation

$$k^2 = k_x^2 + k_y^2 + k_z^2. \tag{6}$$

The boundaries along y and z are assumed to be acoustically hard such that $k_y = m\pi/H$ and $k_z = n\pi/W$. Assuming $p(x,y,z,t) = P(x,y,z)e^{i\omega t}$ leads to

$$P(x,y,z) = \sum_{n=0}^{\infty}\sum_{m=0}^{\infty}\left[A_{nm}^{+}e^{-ik_x x} + A_{nm}^{-}e^{ik_x x}\right]\Psi_{nm}(y,z). \tag{7}$$

where $A_{nm}^{\pm}$ are the reflected and incident mode amplitudes and $\Psi_{nm} = \cos(m\pi y/H)\cos(n\pi z/W)$.

3.2.1 Modal Decomposition

Many investigators [11–14] have utilized mode decompositions in high frequency duct acoustics applications where more than one mode is present. If the HIMIT measurement microphones are used to acquire measurements of $P(x,y,z)$, a linear system,

$$\mathbf{P} = \mathbf{T}\mathbf{A}, \tag{8}$$

can be formed to determine the modal coefficients, where

$$\mathbf{P} = \begin{bmatrix} P(x_1,y_1,z_1) \\ \vdots \\ P(x_I,y_I,z_I) \end{bmatrix} \tag{9}$$

is a vector containing I number of microphone measurements. The transfer matrix is given by

$$\mathbf{T} = \begin{bmatrix} T_{00}^{+}(x_1,y_1,z_1) & \dots & T_{NM}^{+}(x_1,y_1,z_1) & T_{00}^{-}(x_1,y_1,z_1) & \dots & T_{NM}^{-}(x_1,y_1,z_1) \\ \vdots & & \ddots & & & \vdots \\ T_{00}^{+}(x_I,y_I,z_I) & \dots & T_{NM}^{+}(x_I,y_I,z_I) & T_{00}^{-}(x_I,y_I,z_I) & \dots & T_{NM}^{-}(x_I,y_I,z_I) \end{bmatrix} \tag{10}$$

where $T^+_{nm}(x_i, y_i, z_i) = \Psi_{nm}(y_i, z_i)e^{-ik_x x_i}$ and $T^-_{nm}(x_i, y_i, z_i) = \Psi_{nm}(y_i, z_i)e^{ik_x x_i}$, and

$$\mathbf{A} = \begin{bmatrix} A^+_{00} \\ \vdots \\ A^+_{NM} \\ A^-_{00} \\ \vdots \\ A^-_{NM} \end{bmatrix}, \tag{11}$$

is the vector containing the modal amplitudes. The mode NM is the highest cut-on mode present in the HIMIT at the source frequency. The solution of Eqn. (8) for the modal amplitudes is

$$\mathbf{A} = \left[\mathbf{T}^T\mathbf{T}\right]^{-1}\mathbf{T}^T\mathbf{P}. \tag{12}$$

The modal amplitudes are computed in the least squares sense using a singular value decomposition.

3.2.2 HIMIT Impedance Calculation

The relationship between the axial acoustic velocity u_x and acoustic pressure p is determined by the momentum equation in a medium without flow,

$$\rho\frac{\partial u_x}{\partial t} = -\frac{\partial p}{\partial x}, \tag{13}$$

where ρ is the ambient density. Performing a Fourier transform on Eqn. (13) leads to

$$\rho ckU_x = -\frac{\partial P}{\partial x}. \tag{14}$$

Thus, U_x can be expressed as

$$U_x(x, y, z) = \frac{k_x}{\rho ck}\sum_{n=0}^{\infty}\sum_{m=0}^{\infty}\left[A^+_{nm}e^{-ik_x x} - A^-_{nm}e^{ik_x x}\right]\Psi_{nm}(y, z). \tag{15}$$

We will derive the expression for the impedance using the coordinate system established in Fig. 3. The impedance of a locally reacting sample can be computed as the ratio of the acoustic pressure to the normal acoustic particle velocity impinging on the sample,

$$Z = \frac{P}{\mathbf{U}\cdot\mathbf{n}} = -\frac{P}{U_x}. \tag{16}$$

Thus,

$$Z_{nm,nm} = \left(\frac{\rho ck}{k_x}\right)\frac{1 + R_{nm,nm}}{1 - R_{nm,nm}}, \tag{17}$$

where $R_{nm,nm} = A^+_{nm}/A^-_{nm}$ is the reflection factor for the nm mode (A^+_{nm} modes are reflected and A^-_{nm} modes are incident). The normalized specific acoustic impedance is computed using the following equation,

$$\zeta_{nm,nm} = \left(\frac{k}{k_x}\right)\frac{1 + R_{nm,nm}}{1 - R_{nm,nm}}. \tag{18}$$

When multiple modes are present in the HIMIT, care must be taken to compute the impedance using the mode with the most power, since it is difficult to gather accurate data for modes with significantly less power than the dominant mode. Considering only the reflected waves, the intensity is

$$\mathbf{I}^+ \cdot \mathbf{n} = I_x^+(x,y,z) = \frac{1}{2}\mathcal{R}\left[P^+ U_x^{+*}\right], \tag{19}$$

which is related to the power in the duct by

$$\mathcal{P}^+ = \int_0^W \int_0^H I_x^+(x,y,z) dydz. \tag{20}$$

Using the expressions for P and U_x in Eqns. (7) and (15), we get

$$\mathcal{P}^+ = \frac{1}{2}\frac{k_x}{\rho c k}\int_0^W \int_0^H \mathcal{R}\left[\left(\sum_{n=0}^{\infty}\sum_{m=0}^{\infty} A_{nm}^+ e^{-ik_x x}\Psi_{nm}(y,z)\right)\left(\sum_{q=0}^{\infty}\sum_{r=0}^{\infty} A_{qr}^{+*} e^{ik_x x}\Psi_{qr}(y,z)\right)\right] dydz. \tag{21}$$

Due to orthogonality of Ψ, the acoustic power integrates to zero when $nm \neq qr$. The power is also not a function of the axial distance since the exponential terms cancel out. Therefore,

$$\mathcal{P}^+ = \sum_{n=0}^{\infty}\sum_{m=0}^{\infty}\mathcal{P}_{nm}^+ = \sum_{n=0}^{\infty}\sum_{m=0}^{\infty}\frac{1}{2}\frac{k_x}{\rho c k}\mathcal{R}\left[A_{nm}^+ A_{nm}^{+*}\right]\int_0^W\int_0^H \Psi_{nm}^2(y,z)\, dydz. \tag{22}$$

Thus, the power in each mode is

$$\mathcal{P}_{nm}^+ = \frac{\epsilon_{nm}}{2}\frac{k_x}{\rho c k}\mathcal{R}\left[A_{nm}^+ A_{nm}^{+*}\right], \tag{23}$$

where

$$\epsilon_{nm} = \int_0^W\int_0^H \Psi_{nm}^2(y,z)\, dydz = \begin{cases} WH, & \text{if } n=m=0 \\ 0.5WH, & \text{if } n\neq 0 \text{ and } m=0, \text{ or } n=0 \text{ and } m\neq 0 \\ 0.25WH, & \text{if } n\neq 0 \text{ and } m\neq 0. \end{cases} \tag{24}$$

As will be shown in Section 4, impedances computed for the mode with the most power represent the most reliable estimate of the true impedance at the test frequency of interest.

4 Results

The goals of this study are to demonstrate the ability to use data acquired in the HIMIT to accurately educe the impedance of acoustic liners at frequencies up to 6 kHz and at SPLs up to 155 dB. For this phase of the study, these two goals are independently evaluated: full frequency range performance is evaluated at low SPL (120 dB), while high SPL performance is demonstrated at lower frequencies where only plane wave ([0,0] mode) are present. A later investigation is planned to explore the effects of testing simultaneously at both high frequencies and high amplitudes.

The CSQ3 liner was selected for the full-frequency demonstration. As noted earlier, this liner is very linear and is easily predictable using the ZKTL impedance model. This liner has been

previously evaluated in the NIT for frequencies where only plane waves ([0,0] mode) are present. Thus, the first goal of the current study was to demonstrate that the HIMIT could be used to achieve similar results to those predicted with ZKTL and previously educed in the NIT.

The initial portion of the test was conducted at frequencies of 0.5 to 3.0 kHz in 0.5 kHz increments, at an SPL of 120 dB, with each of the rotating plugs set to an angle of zero degrees (measured relative to the axially aligned configuration). In other words, each of the four microphones on a particular wall were aligned in the axial direction. One of the microphones in the rotating plug closest to the sample on the right wall is labeled as Microphone 1 (M1). For this initial test, acoustic pressure data were acquired with M1 sequentially positioned 2.50" and 3.75" from the CSQ3 liner surface.

These data were used with the TMM to determine the surface impedance of the CSQ3 liner. It is important to note that the TMM requires the change in acoustic pressure between the two selected locations but does not require absolute values at either location. Thus, there is no requirement that Microphone 1 (the only microphone used in the TMM) be calibrated, although it clearly must be a properly functioning microphone. However, it is important that the reference microphone (located 0.25" from the liner surface) is calibrated such that we can ensure that the liner is evaluated at the same SPL for each test frequency. For this and all successive tests, the reference microphone was calibrated using an external calibrator provided by the manufacturer.

Figure 4 presents a comparison of three impedance spectra. The first (solid black line) is computed using the ZKTL impedance prediction model. Impedances educed with the TMM are depicted with a red dashed line (based on NIT measurements) and green circles (based on measurements with Microphone 1 in the HIMIT). The NIT results (acquired at 0.1 kHz increments) are nearly identical to the predictions for frequencies up to 3 kHz (the full range of the NIT), with noticeable deviations at frequencies very near antiresonance (frequencies where the reactance crosses zero with negative slope). It is perhaps worth noting that significant variability in the impedance at this frequency results in very limited impact on the amount of sound absorption provided by the liner. As a result, the differences between measured and predicted impedances for frequencies near antiresonance are of minimal concern. While the HIMIT data (M1) is more sparse, the results compare favorably with those measured in the NIT. Together, these results confirm the predictability of the CSQ3 liner and also demonstrate that the single microphone in the HIMIT can be used to accurately determine the impedance for plane-wave frequencies.

In contrast to the TMM, it is critical that all of the measurement microphones are calibrated for use with the modal analysis and impedance calculation approach described in Section 3.3.2. An in situ microphone calibration process is implemented based on TMM results at 1 kHz. This frequency is at resonance (frequency where reactance crosses zero with positive slope), where the liner provides near maximum sound absorption and the impedance comparison is excellent. If the SPL and phase at the reference microphone and the liner impedance at an individual frequency are known, the acoustic pressure standing wave pattern (SPL and phase) throughout the waveguide can be computed. Figure 5 presents this standing wave pattern, and includes vertical dashed lines at the axial locations where each of the microphones are initially located. Observe that the SPL and phase are 120 dB and 0 deg at the reference microphone location (at 0.25"). The SPL represents the value set by adjusting the excitation voltage to the acoustic drivers and the phase is arbitrarily chosen as the frame of reference (i.e., all phases are relative to that measured at this location).

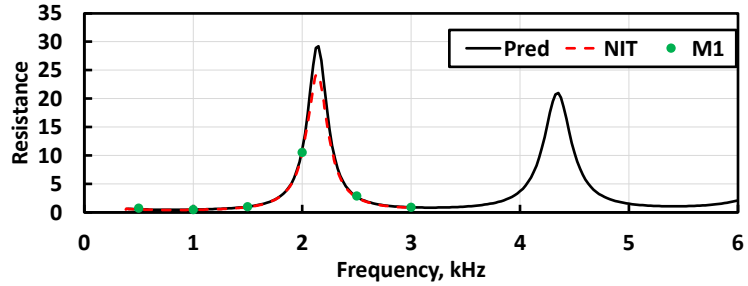

(a) Normalized Resistance.

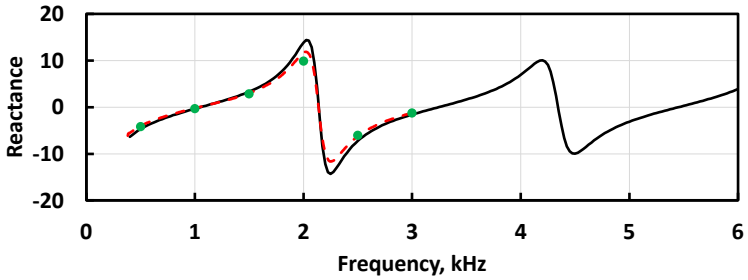

(b) Normalized Reactance.

Figure 4: Comparison of impedance spectra predicted with ZKTL and educed using the TMM (NIT and HIMIT Microphone 1) for CSQ3 calibration liner.

For the calibration process, the four rotating plugs are oriented such that all microphones are perfectly aligned in the axial direction (four on each wall). As a result, there are two microphones in each of the axial planes denoted with vertical dashed lines except at $x = 0.25''$, where the reference microphone is located. Therefore, this standing pattern represents the true SPL and phase (relative to the signal measured by the reference microphone) at each of the eight measurement microphone locations. The difference between these true values and those measured with each of the measurement microphones can then be used as microphone-dependent calibration factors (both magnitude and phase) in successive measurements. As noted earlier, these measurement microphones have a frequency-independent response over the full frequency range of interest. Thus, these calibration factors (per microphone) apply for all successive data regardless of the test frequency that is used.

For the second portion of this initial test, rotating plugs RP1 and RP4 were set to 30 degrees and rotating plugs RP2 and RP3 were set to 60 degrees, i.e., none of the microphones were along the spanwise centerline of the wall. Data were then acquired at frequencies of 0.5 to 6.0 kHz in 0.5 kHz increments, again at an SPL of 120 dB. The correction factors computed via the in situ process noted above are used to determine the true complex acoustic pressures at each of the microphone locations, and the resultant data are processed via the modal approach described in Section 3. As noted in that description, this process results in an impedance spectrum for each mode that is cut on in the HIMIT (which increases in number as the frequency increases).

Figure 6 presents the results of this analysis, with the impedance attributed to each mode depicted with open circles. Note that the data for each mode are only presented at the frequencies for which that particular mode is cut on ([0,0] mode is always cut on, [1,0] and [0,1] modes cut on at about 3.4 kHz, and [1,1] mode cuts on near 4.8 kHz). Two features are readily apparent in these

results. First, the results for frequencies up to 3 kHz compare very favorably with those educed using the TMM approach with Microphone 1 data. Although the results for the higher frequencies generally follow the predicted curves, the comparisons are much less favorable.

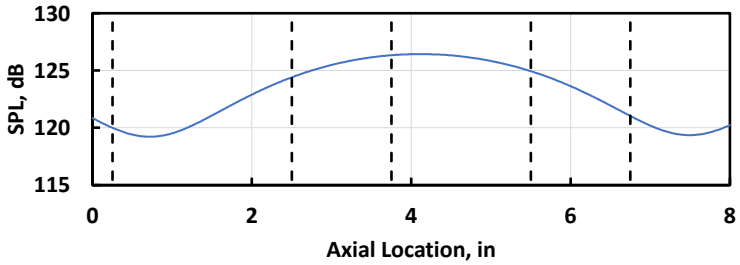

(a) Predicted axial SPL distribution.

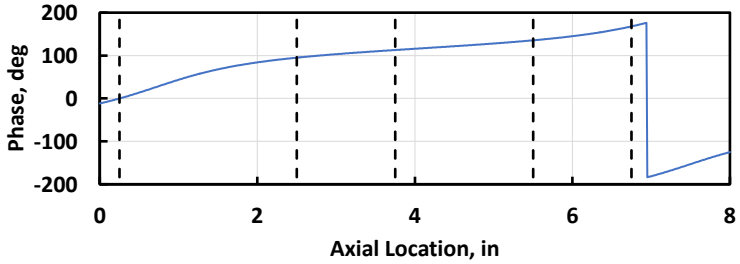

(b) Predicted axial phase distribution.

Figure 5: Predicted axial SPL and phase distributions for the CSQ3 liner at a test frequency of 1 kHz. Vertical lines depict axial locations of each HIMIT microphones.

It is hypothesized that this variability in impedances educed using the modal approach is due to insufficient power in the respective modes. Hence, it is conjectured that the mode with the maximum acoustic power should be expected to provide the best estimate of the liner impedance. Table 1 provides a listing of the impedances ($\zeta = \theta + i\chi$) and sound power level educed for each mode that is cut on for a particular frequency (i.e., cells are left blank where a specific mode is cut off). The results for the mode containing the highest sound power level are depicted in red font, as these are the results that are assumed to be the best estimate of the liner impedances (on a per frequency basis). Figure 7 presents impedance spectra (green squares) taken from these maximum power readings. Observe that this results in an excellent comparison, albeit with small deviations at frequencies near antiresonance. While the maximum-power approach for choosing the 'proper' educed impedance will continue to be assessed, it is deemed acceptable for current usage. Also, these results demonstrate the capability of the HIMIT to acquire quality data up to 6 kHz.

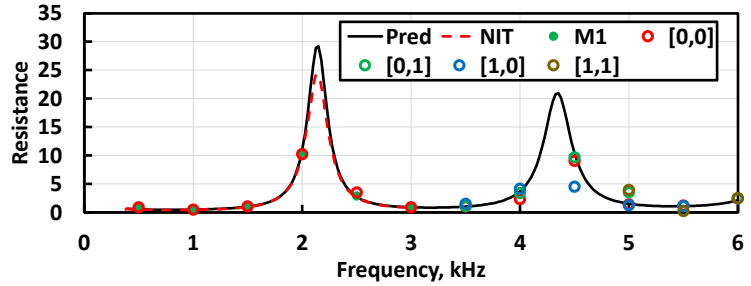

(a) Normalized Resistance.

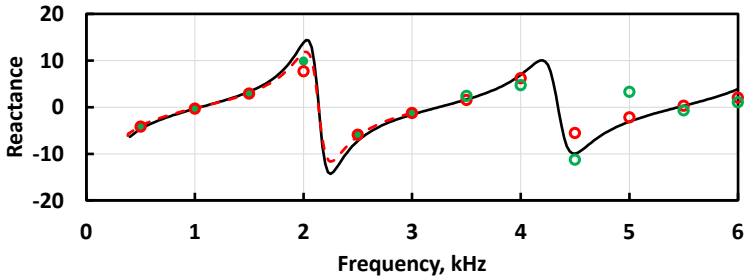

(b) Normalized Reactance.

Figure 6: Replication of Figure 4 with impedances educed using the modal approach included.

Table 1: Impedance and sound power level as a function of mode order.

	Impedance per mode								Power Level per mode			
	[0,0]		[1,0]		[0,1]		[1,1]		[0,0]	[1,0]	[0,1]	[1,1]
Freq, kHz	θ	χ	θ	χ	θ	χ	θ	χ	dB	dB	dB	dB
0.5	0.90	-4.14							88.5			
1.0	0.48	-0.27							97.6			
1.5	1.02	2.93							88.6			
2.0	10.23	7.71							88.3			
2.5	3.50	-5.91							89.2			
3.0	0.90	-1.22							93.8			
3.5	1.03	1.54	1.49	1.83	1.09	2.46			91.4	73.9	71.5	
4.0	2.30	6.21	4.16	5.17	3.42	4.72			75.0	81.3	83.3	
4.5	9.07	-5.54	4.51	-4.23	9.68	-11.22			90.7	69.7	67.4	
5.0	1.41	-2.14	1.25	-2.26	3.56	3.32	3.93	-2.17	91.2	83.2	71.6	73.2
5.5	1.22	0.36	1.09	0.72	1.09	-0.65	0.21	-1.64	97.4	90.0	80.6	57.9
6.0	-0.86	2.04	2.45	3.10	2.47	1.08	2.46	1.33	74.8	86.0	65.9	66.7

The last objective is to evaluate the ability of the HIMIT to acquire quality data at higher SPLs, albeit at frequencies where only the plane wave ([0,0] mode) is cut on (up to 3 kHz). To do so,

another test was conducted with two samples (CSQ3 and GE01) at frequencies of 0.5 to 3.0 kHz in 0.5 kHz increments, with the SPL increased to 155 dB. It should be noted that the HIMIT is capable of achieving higher SPLs over a large portion of the frequency range, but there are dropouts at selected narrow frequency bands. The desire for this test was to ensure that all test frequencies were evaluated at the same SPL, which led to the choice of 155 dB. As these data were to be processed with the TMM approach, data were acquired with the rotating plugs sequentially set to zero and 180 degrees.

One concern about testing at this higher level is the possibility of nonlinear acoustic propagation. If a single tone (sine wave) is emitted at a sufficiently high SPL into a sufficiently long waveguide, the time history of that tone will morph from a sine wave to an 'N-wave', i.e., the sound will disperse into higher harmonics. Thus, the initial goal is to determine whether the duct length is sufficient for this to negatively affect the results. The CSQ3 calibration liner is used for this assessment, as it is very linear (the impedance is independent of SPL) and predictable.

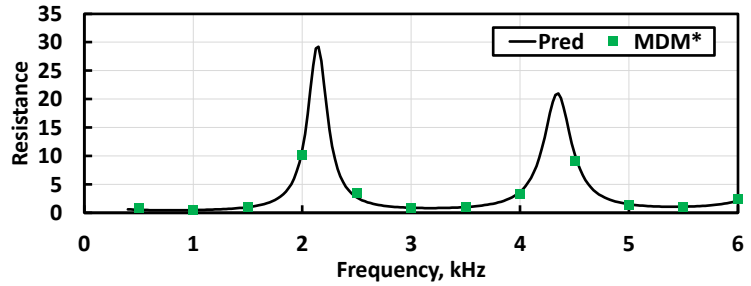

(a) Normalized Resistance.

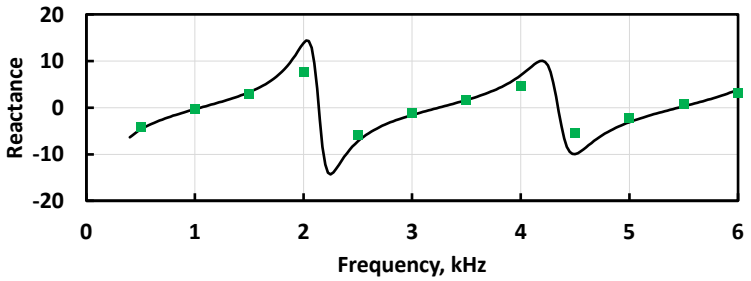

(b) Normalized Reactance.

Figure 7: Comparison of impedance spectra predicted with ZKTL and those educed using the modal approach for the mode with the highest power.

Figure 8 presents a comparison of the predicted and educed impedance spectra for the CSQ3 liner. Impedances educed in the NIT with an SPL of 120 dB are depicted with a red dashed line, while those educed using Microphone 1 in the HIMIT are depicted with blue circles. Recall that when the HIMIT was set to an SPL of 120 dB, the results compared very favorably to the prediction and NIT data. The results for an SPL of 155 dB also compare favorably with the earlier data. As noted earlier, significant nonlinear propagation would cause the SPL at the test frequency to be reduced because some of the energy would be transferred to higher harmonics. Also, the amount of energy transfer would vary with axial location. As a result, the educed impedance would be

altered. The fact that the impedance is virtually unaffected by the increase in SPL indicates that nonlinear propagation effects are minimal, at least for this frequency range. This confirms that the HIMIT can be used to acquire high amplitude data with confidence. As noted earlier, later tests are planned to extend this evaluation to higher frequencies.

Similar data were acquired with the conventional perforate-over-honeycomb liner (GE01), which is known to be nonlinear. Two sets of data were acquired in the NIT with a frequency increment of 0.1 kHz, at SPLs of 120 and 140 dB. As expected, the normalized resistance increases with SPL for this weakly nonlinear liner. Although the data acquired in the HIMIT is more sparse, a much more significant increase in resistance is observed when the SPL is increased to 155 dB. The normalized reactance spectra are also as expected., with a slight flattening of the curve as the SPL is increased. The results for both of these liners follow the expected trends, thus providing confidence that the HIMIT can be used to acquire quality data at high amplitudes - at least up to 155 dB.

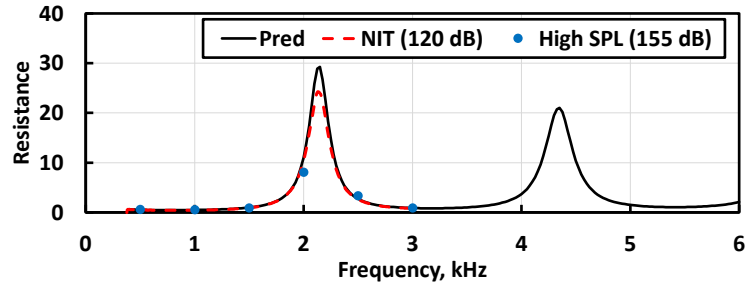

(a) Normalized Resistance.

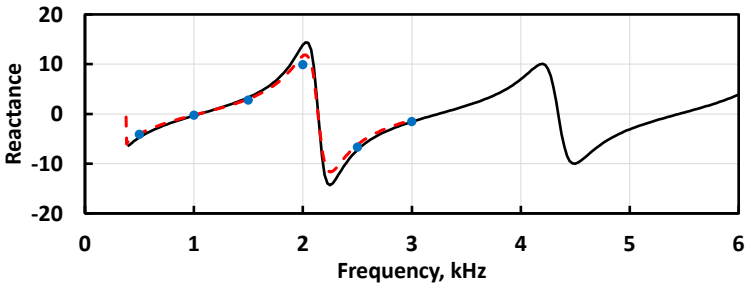

(b) Normalized Reactance.

Figure 8: Comparison of impedance spectra predicted with ZKTL and those educed using the TMM (NIT and HIMIT Microphone 1) for the CSQ3 liner.

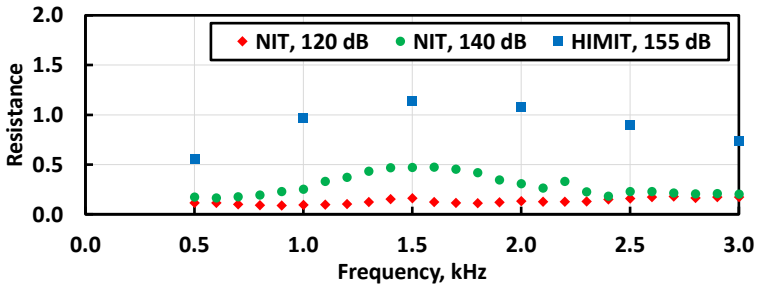

(a) Normalized Resistance.

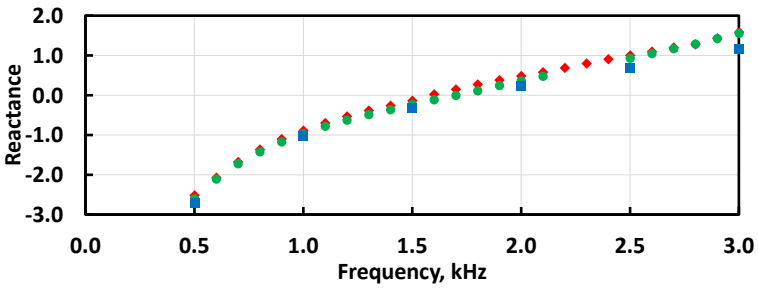

(b) Normalized Reactance.

Figure 9: Comparison of impedance spectra educed using the TMM (NIT and HIMIT Microphone 1) for the GE01 liner.

5 Concluding Remarks

The NASA Langley Research Center Liner Technology Facility has recently brought a new test rig online for evaluation of acoustic liners at frequencies up to 6 kHz and sound pressure levels up to 155 dB. This test rig, labeled the High Intensity Modal Impedance Tube (HIMIT), was evaluated with the use of two acoustic liners, one linear and one nonlinear. Impedances educed from data acquired in the HIMIT were shown to compare favorably with those predicted via a transmission line model based on Zwikker and Kosten's propagation analysis and with those educed in the NASA Langley Normal Incidence Tube. These results confirm that the HIMIT can be used with confidence for the evaluation of acoustic liners over these frequency and sound pressure level ranges. Future plans are to extend this evaluation to evaluate both test regimes simultaneously (i.e., high amplitude and high frequency). Also, a number of additional liners will be evaluated over a wide range of frequencies and amplitudes.

References

1. Lympany, S. V., Karon, A. Z., Wadsworth, M. L., Funk, R., and Ahuja, K. K., "An Experimental Facility for Measuring the Acoustic Reflection and Transmission of Higher-Order Modes in Heated Flows, Part 1: Design and Methodology," AIAA Paper 2018-3133, June 2018.

2. Khodashenas, N. S., Bodén, H., and Boij, S., "Experimental investigation for determination of non-linear properties of perforated plates for tonal, multi tone and random excitation," AIAA Paper 2021-2267, June 2021.

3. Palani, S., Murray, P., McAlpine, A., Knepper, K., and Richter, C., "Assessment of novel acoustic liners for aero-engine applications with sheared mean flow," AIAA Paper 2022-2900, June 2022.

4. Chung, J. Y. and Blaser, D. A., "Transfer function method of measuring in-duct acoustic properties: I. Theory," *Journal of Acoustical Society of America*, Vol. 68, 1980, pp. 907–921.

5. Jones, M. G. and Stiede, P. E., "Comparison of Methods for Determining Specific Acoustic Impedance," *Journal of the Acoustical Society of America*, Vol. 101, No. 5, May 1997, pp. 2694–2704.

6. Parrott, T. L. and Jones, M. G., "Assessment of NASA's Aircraft Noise Prediction Capability, Chapter 6: Uncertainty in Acoustic Liner Impedance Measurement and Prediction," NASA TP 2012-215653, July 2012.

7. Jones, M. G., Parrott, T. L., and Watson, W. R., "Uncertainty and Sensitivity Analyses of a Two-Parameter Impedance Prediction Model," AIAA Paper 2008-2928, May 2008.

8. Zwikker, C. and Kosten, C., *Sound absorbing materials*, Elsevier Publishing Company, 1949.

9. Parrott, T. L. and Jones, M. G., "Parallel-Element Liner Impedances for Improved Absorption of Broadband Sound in Ducts," *Noise Control Engineering Journal*, Vol. 43, No. 6, Nov. 1995.

10. Jones, M. G., Howerton, B. M., and Ayle, E., "Evaluation of Parallel-Element, Variable-Impedance, Broadband Acoustic Liner Concepts," AIAA Paper 2012-2194, June 2012.

11. Jang, S.-H. and Ih, J.-G., "On the multiple microphone method for measuring in-duct acoustic properties in the presence of mean flow," *Journal of the Acoustical Society of America*, Vol. 103, No. 3, March 1998, pp. 1520–1526.

12. Schultz, T., Cattafesta, L. N., and Sheplak, M., "Modal decomposition method for acoustic impedance testing in square ducts," *Journal of the Acoustical Society of America*, Vol. 120, No. 6, March 2006, pp. 3750–3758.

13. Gerhold, C., Cabell, R., and Brown, M., "Development of an Experimental Rig for Investigation of Higher Order Modes in Ducts," AIAA Paper 2006-2637, May 2006.

14. Boucheron, R., "Modal decomposition method in rectangular ducts in a test-section of a cavitation tunnel with a simultaneous estimate of the effective wall impedance," *Ocean Engineering*, Vol. 209, 2020, pp. 107491.

REPORT DOCUMENTATION PAGE

Form Approved
OMB No. 0704–0188

1. REPORT DATE *(DD-MM-YYYY)*	2. REPORT TYPE	3. DATES COVERED *(From - To)*
01-12-2022	Technical Memorandum	

4. TITLE AND SUBTITLE
Implementation of the NASA High Intensity Modal Impedance Tube

5a. CONTRACT NUMBER

5b. GRANT NUMBER

5c. PROGRAM ELEMENT NUMBER

6. AUTHOR(S)
Michael G. Jones, Alexander N. Carr, and Douglas M. Nark
NASA Langley Research Center, Hampton, VA 23681
and
Lawrence E. Becker
Analytical Services & Materials, Hampton, VA 23681

5d. PROJECT NUMBER

5e. TASK NUMBER

5f. WORK UNIT NUMBER

7. PERFORMING ORGANIZATION NAME(S) AND ADDRESS(ES)
NASA Langley Research Center
Hampton, Virginia 23681-2199

8. PERFORMING ORGANIZATION REPORT NUMBER
L–xxxx

9. SPONSORING/MONITORING AGENCY NAME(S) AND ADDRESS(ES)
National Aeronautics and Space Administration
Washington, DC 20546-0001

10. SPONSOR/MONITOR'S ACRONYM(S)
NASA

11. SPONSOR/MONITOR'S REPORT NUMBER(S)
NASA/TM–20220017773

12. DISTRIBUTION/AVAILABILITY STATEMENT
Unclassified-Unlimited
Subject Category 64
Availability: NASA STI Program (757) 864-9658

13. SUPPLEMENTARY NOTES
An electronic version can be found at http://ntrs.nasa.gov.

14. ABSTRACT

15. SUBJECT TERMS
liner, acoustic impedance

16. SECURITY CLASSIFICATION OF:			17. LIMITATION OF ABSTRACT	18. NUMBER OF PAGES	19a. NAME OF RESPONSIBLE PERSON
a. REPORT	b. ABSTRACT	c. THIS PAGE			STI Information Desk (help@sti.nasa.gov)
U	U	U	UU	21	19b. TELEPHONE NUMBER *(Include area code)* (757) 864-9658